Chaotic Modeling and Simulation (CMSIM) 1: 241–256, 2012

Wave Fractal Dimension as a Tool in Detecting Cracks in Beam Structures

Chandresh Dubey[1] and Vikram Kapila[2]

[1] Polytechnic Institute of NYU, 6 Metrotech Center, Brooklyn, New York (E-mail: cdubey01@students.poly.edu)
[2] Polytechnic Institute of NYU, 6 Metrotech Center, Brooklyn, New York (E-mail: vkapila@poly.edu)

Abstract. A chaotic signal is used to excite a cracked beam and wave fractal dimension of the resulting time series and power spectrum are analyzed to detect and characterize the crack. For a single degree of freedom (SDOF) approximation of the cracked beam, the wave fractal dimension analysis reveals its ability to consistently and accurately predict crack severity. For a finite element simulation of the cracked cantilever beam, an analysis of spatio-temporal response using wave fractal dimension in frequency domain reveals distinctive variation vis-à-vis crack location and severity. Simulation results are experimentally validated.
Keywords: Chaotic excitation, Chen's oscillator, Wave fractal dimension.

1 Introduction

Vibration-based methods for crack detection in beam type structures continue to attract intense attention from researchers. Most often these methods use external forcing input, e.g., harmonic input, to cause the structure to vibrate. Typical vibration-based crack detection methods exploit modal analysis techniques to determine changes in beam's natural frequency [4,11,13] and relate these changes to the crack severity and in some cases to crack location [17,23]. To quantify the crack depth and to detect crack location, vibration-based crack detection methods employ a variety of characterizing parameters, such as natural frequency [11], mode shape [19], mechanical impedance [2], statistical parameters [22], etc. In recent research, wave fractal dimension, originally introduced by Katz [12] to characterize biological signals, has been used to detect the severity and location of crack in beam [7] and plate structures [8].

Over the last decade, progress in chaos theory has led several researchers to consider the use of chaotic excitation in vibration-based crack detection [15,18]. A majority of these efforts necessitate the reconstruction of a chaotic attractor from the time series data corresponding to the vibration response of the structure [15,18]. Unfortunately, the reconstruction of a chaotic attractor is often tedious and may not always yield satisfactory results for crack detection even in

Received: 20 July 2011 / Accepted: 30 December 2011

ISSN 2241-0503

the SDOF approximation case. To detect and characterize cracks, the current chaos-based crack detection methods use a variety of chaos and statistics-based parameters, such as correlation dimension [18], Hausdorff distance [18], average local attractor variance ratio [15], etc. In this paper, we study the use of wave fractal dimension as a characterizing parameters to predict the severity and location of a crack in a beam that is made to vibrate using a chaotic input.

2 Beam Excitation Methods

In this section, we consider three methods to excite the cracked beam. We begin by producing and analyzing the beam response to a non-zero initial condition which facilitates our understanding of the behavior of wave fractal dimension as a characterizing parameter for crack detection. We consider a unit displacement initial condition. Various references [16,22] have already indicated various reasons for the wide use of harmonic input in vibration-based crack detection. Thus, we next consider the use of both sub-harmonic ($\omega < \omega_n$) and super-harmonic ($\omega > \omega_n$) inputs to vibrate the cracked beam model and study its behavior. Finally, we use the chaotic solution of autonomous dissipative flow type Chen's attractor [20] as an input excitation force to vibrate the SDOF model of cracked beam. The Chen's system in state space form is expressed as

$$\dot{y_1} = a_1(y_2 - y_1), \quad \dot{y_2} = (a_3 - a_1)y_1 - y_1y_3 + a_3y_2, \quad \dot{y_3} = y_1y_2 - a_2y_3, \quad (1)$$

where a_1, a_2, and a_3 are constant parameters. Figure 1 shows the time series y_1 and the 2D phase portrait of Chen's system corresponding to a chaotic solution. For the indicated values of constants a_1, a_2, and a_3 (see Figure 1), the solution y_1 is expected to be non-periodic. We restricted our attention to Chen's system because its solutions y_1 and y_2 are approximately symmetric about the time axis, producing the mean of ≈ 0. Furthermore, in a detailed analysis of several popular chaotic attractors [20], we found that the Chen's system produced one of the largest wave fractal dimension (see Figure 2). Moreover, our analysis has revealed that chaotic attractors possessing these two properties produce large changes in wave fractal dimension with increasing or decreasing crack depths. These advantages will become more apparent in the following sections.

3 Wave Fractal Dimension

Waveforms are common patterns that arise frequently in scientific and engineering phenomena. A waveform can be produced by plotting a collection of ordered (x, y) pairs, where x increases monotonically. The concept of wave fractal dimension [12] is used to differentiate one waveform from another.

For waveforms, produced using a collection of ordered point pairs (x_i, y_i), $i = 1, \ldots, n$, the total length, L, is simply the sum of the distances between successive points, i.e., $L = \sum_{i=1}^{n-1} \sqrt{(x_{i+1} - x_i)^2 + (y_{i+1} - y_i)^2}$. Moreover, the diameter d of a waveform is considered to be the farthest distance between the

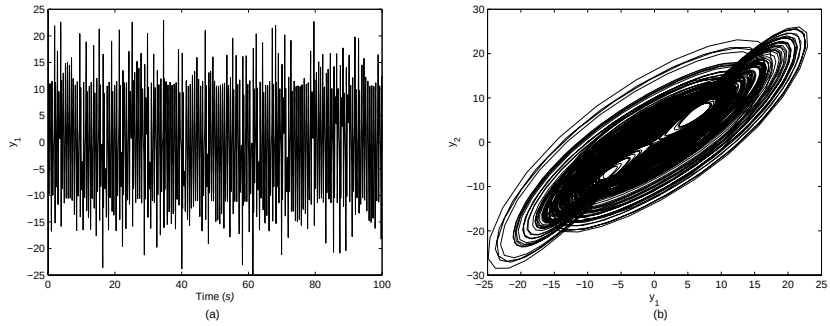

Fig. 1. The chaotic input (Chen's attractor) with $a_1 = 35$, $a_2 = 3$, $a_3 = 28$, $y_1(0) = -10$, $y_2(0) = 0$, and $y_3(0) = 37$. (a) Time series of y_1 and (b) phase portrait projected onto the (y_1, y_2) plane.

starting point (corresponding to $n = 1$) and some other point (corresponding to $n = i$, $i = 2, \ldots, n$), of the waveform, i.e., $d = \max_{i=2,\ldots,n} \sqrt{(x_i - x_1)^2 + (y_i - y_1)^2}$. Next, by expressing the length of a waveform L and its diameter d in a standard unit, which is taken to be the average step α of the waveform, the wave fractal dimension can be expressed as [12]

$$D = \frac{\log(L/\alpha)}{\log(d/\alpha)} = \frac{\log(n)}{\log(n) + \log(d/L)}, \tag{2}$$

where $n = L/\alpha$, denotes the number of steps in the waveform. We use (2) to estimate the wave fractal dimension.

Using (2), wave fractal dimension is calculated for various chaotic attractors and results are shown in Figure 2 only for one waveform (y_1, y_2 or y_3) of each attractor having maximum wave fractal dimension. Waveforms are normalized before calculating wave fractal dimension to maintain parity among various attractors. It is found that Chen's attractor has the largest fractal dimension and this was the reason for using Chen's attractor in current study.

4 Modeling of a Cracked Beam as a SDOF System with Force Input

Following [1,18], a cracked beam is modeled as a SDOF switched system which emulates the opening and closing of the surface crack by switching the effective stiffness $k_s = k - \Delta k$, where k is the stiffness of the beam without crack, k_s is stiffness during stretching and Δk is stiffness difference. For a SDOF model with a relatively small crack, the ratio of Δk to k is equal to the ratio of the crack depth a to the thickness h of the beam [1,18]. Next, we consider that the y_1 solution of (1) is applied as a force to the mass of the SDOF system. The equations of motion for this piecewise continuous SDOF system are

$$\begin{aligned} M\ddot{x} + c\dot{x} + kx &= F(t), \qquad \text{for } x \geq 0, \\ M\ddot{x} + c\dot{x} + k_s x &= F(t), \qquad \text{for } x < 0, \end{aligned} \tag{3}$$

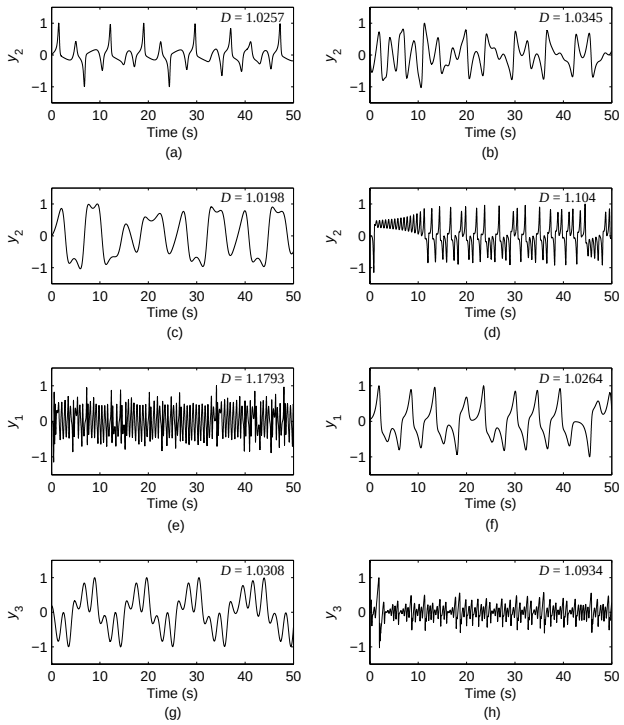

Fig. 2. Wave fractal dimension of chaotic attractor waveforms. (a) Vanderpol attractor y_2 component; (b) Ueda attractor y_2 component; (c) Duffing's two well attractor y_2 component; (d) Lorenz attractor y_2 component; (e) Chen's attractor y_1 component; (f) ACT attractor y_1 component; (g) Chua's attractor y_3 component; and (h) Burkeshaw attractor y_3 component.

where M is the mass of the cantilever beam, c is the damping coefficient, and x is the displacement of the beam. The physical parameters of the problem data used in our simulations are as follows: mass $m = 0.18$ kg, nominal stiffness $k = 295$ N/m, and damping $c = 0.03$ Ns/m.

5 SDOF Results

For the three excitation methods of Section 2, the system responses for the SDOF model of section 4 are recorded and analyzed to carefully examine the influence of different excitation methods and signal characteristics on the behavior of wave fractal dimension (2). Moreover, we consider alternative ways to efficiently compute the wave fractal dimension.

5.1 SDOF results of wave fractal dimension for non-zero initial condition

We begin by simulating the SDOF system of (3) with a unit displacement initial condition and $F(t) = 0$, for $t \geq 0$. The simulation is performed for various

values of small crack depths and the resulting time series data is provided in Figure 3. In each case, the vibration starts with unit displacement and eventually settles to zero due to damping. Even though all the curves look quite similar, the damped vibration frequency decreases with increasing crack depth [6]. Next, for each time series, we compute the corresponding wave fractal dimension and plot normalized crack depth versus the wave fractal dimension in Figure 4, which shows the wave fractal dimension decreases with increasing crack depth. As indicated above, increasing crack depth leads to lowering of the waveform frequency, thereby reducing the wave fractal dimension. Furthermore, note that the trend shown in Figure 4 is quite monotonic and can be used to detect small cracks. Unfortunately, the rate of change of wave fractal dimension vis-à-vis crack depth is very small.

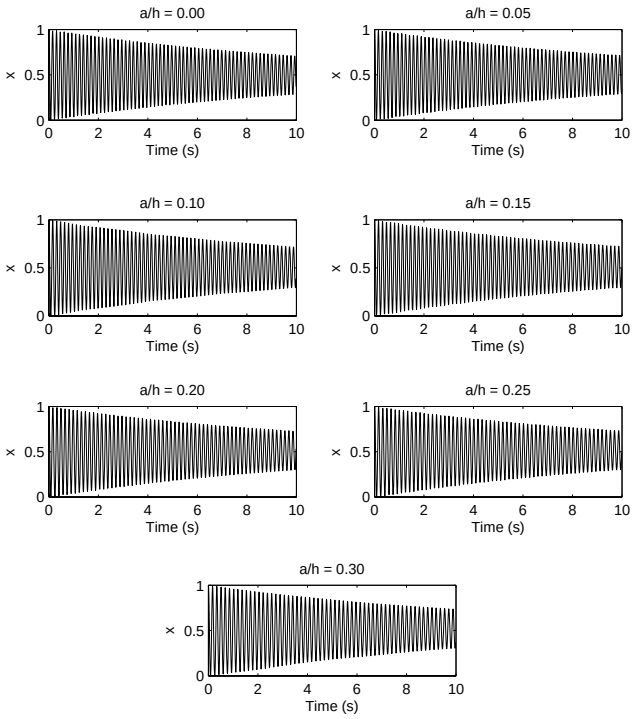

Fig. 3. Time response of the SDOF system to non-zero initial displacement

5.2 SDOF results of wave fractal dimension with harmonic input

For a SDOF model (3) emulating a cracked beam, the natural frequency of the resulting model depends on the crack depth and will not be known prior to crack characterization. Thus, we consider the use of sub-harmonic ($\omega < \omega_n$) and super-harmonic ($\omega > \omega_n$) force inputs to vibrate the SDOF model for various values of crack depths. Figure 5 provides the resulting time series

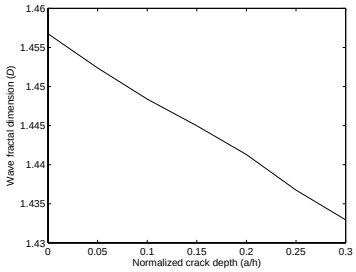

Fig. 4. Change of the wave fractal dimension with normalized crack depth for unit initial displacement

plots for the sub-harmonic input case with various normalized crack depths. Following the initial transient response, in each plot, a steady state sinusoidal response is observed. Moreover, these responses reveal that the amplitude of the output waveform increases with increasing crack depth.

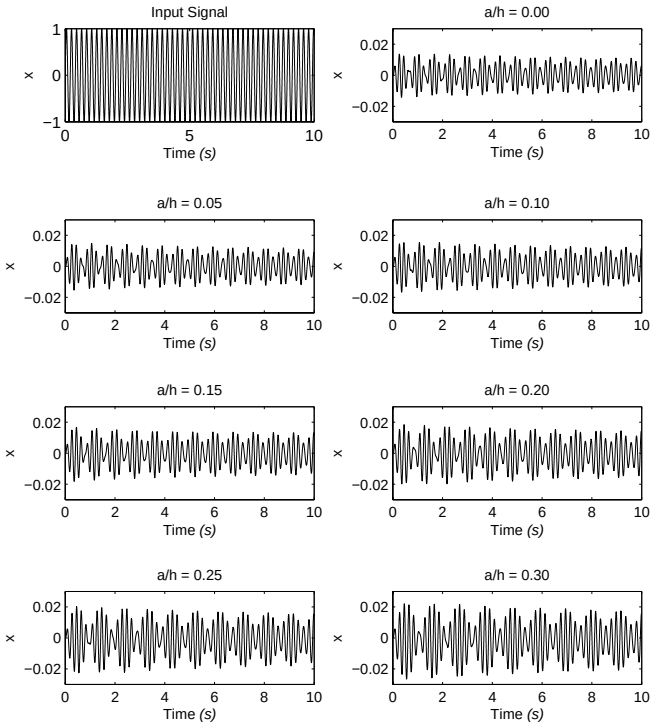

Fig. 5. Time response of the SDOF system to sub-harmonic ($\omega < \omega_n$) input

Next, for each time series of Figure 5, we compute the corresponding wave fractal dimension and plot normalized crack depth versus the wave fractal dimension in Figure 6(a), which shows that the wave fractal dimension mono-

tonically increases with increasing crack depth. Note that, as indicated above, increasing crack depth leads to increasing amplitude of the waveform, leading to an increase in the wave fractal dimension. Next, we apply a super-harmonic ($\omega > \omega_n$) forcing input to vibrate the SDOF model for various values of crack depths. From the resulting time series, we compute the corresponding wave fractal dimension and plot normalized crack depth versus the wave fractal dimension in Figure 6(b), which shows that the wave fractal dimension monotonically decreases with increasing crack depth. The results of this subsection indicate that in order to accurately predict the crack depth, we need to know the approximate natural frequency of the cracked system so that the correct graph (Figure 6(a) versus 6(b)) can be used. This is not very satisfactory since, as noted above, the natural frequency of the cracked beam depends on the crack depth and is not known *a priori*.

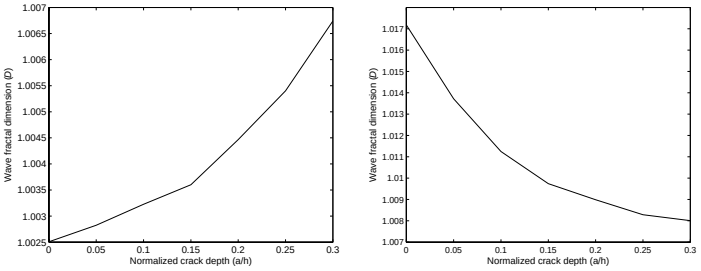

(a) (b)

Fig. 6. Change of the wave fractal dimension with normalized crack depth for (a) sub-harmonic ($\omega < \omega_n$) and (b) super-harmonic ($\omega > \omega_n$) input

5.3 SDOF results of wave fractal dimension with chaotic input

We now consider the application of the chaotic forcing input of section 2 to vibrate the SDOF model for various values of crack depths. Figure 7 provides the resulting time series plots for the chaotic input with various normalized crack depths. Since the resulting waveforms are non-periodic, no obvious trends can be discerned from these plots. Next, for each time series of Figure 7, we compute the corresponding wave fractal dimension and plot normalized crack depth versus the wave fractal dimension in Figure 8, which shows that the wave fractal dimension monotonically increases with increasing crack depth. Note that, in contrast to the harmonic forcing input case, when using a chaotic excitation we do not need *a priori* knowledge of the natural frequency of the cracked beam. This feature is facilitated by the fact that the chaotic excitation signal has a broad frequency content.

Since wave fractal dimension is a characteristic of the waveform only, we consider the wave fractal dimension analysis of the time series of Figure 7 in frequency domain. To do so, we use the Fast Fourier Transform (FFT) [10]

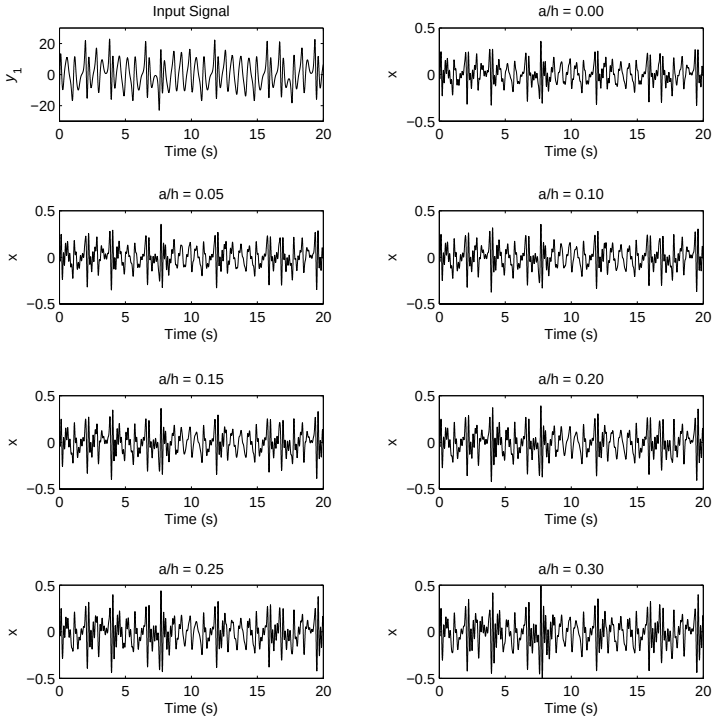

Fig. 7. Time response of the SDOF system with chaotic input

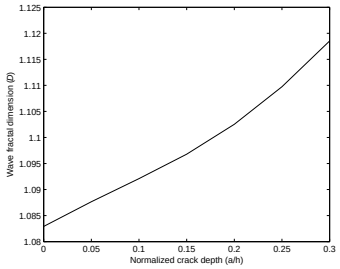

Fig. 8. Change of the wave fractal dimension with normalized crack depth for chaotic input

technique to convert the time domain data of Figure 7 to frequency domain. The resulting frequency domain data in Figure 9 provides the power spectrum of the response of the SDOF cracked beam. Whereas the time response plots of Figure 7 do not reveal any trend, the power spectrum illustrates that the portion of FFT in the vicinity of beam's natural frequency ω_n experiences significant changes. Thus, we now concentrate in the neighborhood of ω_n as our window for computing the wave fractal dimension. Using this technique, in Figure 10(a), we plot normalized crack depth versus the wave fractal dimension for the windowed waveforms of Figure 9. From Figure 10(a), we observe that

the wave fractal dimension monotonically increases with increasing crack depth and this curve exhibits a significant rate of change. Thus, in the following analysis, we use the wave fractal dimension of power spectrum as a natural choice for crack detection and crack characterization.

Finally, we also plot wave fractal dimension versus normalized crack depth plots for power spectrum constructed from the FFT of non-zero initial condition response and the harmonic input response corresponding to Figures 3 and 5, respectively. The resulting plots are provided in Figures 10(b) and 10(c) and demonstrate that the frequency domain wave fractal dimension analysis is an effective way to characterize crack depth in a SDOF system.

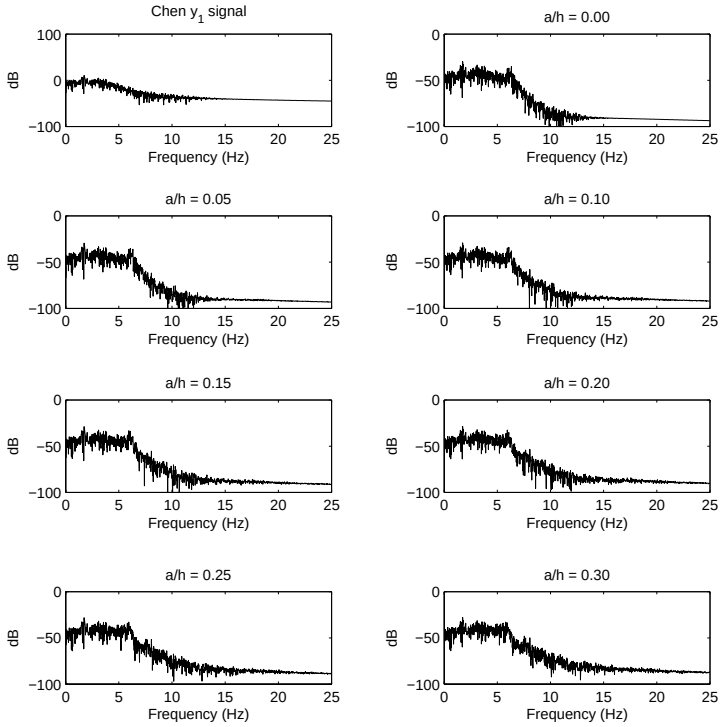

Fig. 9. Power spectrum of the time response of SDOF system with chaotic input

6 Continuous Model Case

We now extend the results of section 5 to the continuous model case. To do so, as in [19,21], we consider a continuous model of the dynamical behavior of the beam with a surface crack in two parts. Specifically, when the beam moves away from the neutral position so that the crack remains closed, the beam behaves as a typical continuous beam [6,19,21]. However, when the beam moves in the other direction from the neutral position, causing the crack to open, the

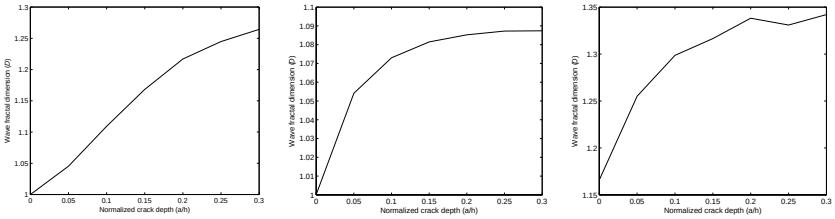

(a) (b) (c)

Fig. 10. Frequency domain change of the wave fractal dimension with normalized crack depth for (a) chaotic input, (b) unit initial displacement, and (c) harmonic input

resulting dynamics require the modeling of crack with a rotational spring whose stiffness is related to the crack depth [2,6,19,21].

Next, we used the ANSYS software [14] to simulate the dynamics of a cracked beam under external excitation. We modeled the beam as a 2-D elastic object using a *beam3* element [14] which has tension, compression, and bending capabilities. The crack is simulated by inserting a torsional spring at the location of the crack and using the mathematical model described in [2,6,19,21]. The torsional spring is modeled using a *combin14* element [14] which is a spring-damper element used in 1-D, 2-D, and 3-D applications. In our finite element (FE) model, we used the *combin14* element as a pure spring with 1-D (i.e., torsional) stiffness since the model of [2,6,19,21] does not consider damping. The physical characteristics of the beam used in our FE model are as follows: material–Plexiglass, length–500 mm, width–50 mm, thickness–6 mm, modulus of elasticity–3300 MPa, density–1190 kg/m^3, and Poisson's ratio–0.35. This FE model was validated [6] by comparing the natural frequencies resulting from the FE simulations versus the natural frequencies computed in Matlab [5] for the dynamic model of [6,19,21].

Next, we apply force input to the FE model using the time series y_1 of (1). In particular, using MATLAB, we simulate (1) and save $15,000$ time steps of y_1 time series, which is applied as force input at 40 mm from the fixed end in ANSYS. The FE simulation is used to produce and record spatio-temporal responses for each node (corresponding to discretized locations along the beam span). The resulting data is imported in MATLAB for a detailed wave fractal dimension analysis.

To detect the presence of a crack in the beam, we only consider the time series data corresponding to the beam tip displacement. The time series for tip displacement is converted to the frequency domain using the FFT. The resulting power spectrum plot is provided in Figure 11 for various sizes of cracks located at $L_1 = 0.2L$. From Figure 11, we observe significant changes around 6.4Hz which corresponds to the first fundamental frequency of the beam. These changes in the power spectrum are due to changes in crack depth at $L_1 = 0.2L$. To characterize the changes in crack depth, we now compute and plot the wave fractal dimension for cracks at various location along the beam. For example, Figure 12 provides wave fractal dimension curves for a crack

located at $L_1 = 0.2L$ and, alternatively, at $L_1 = 0.4L$. We term these curves as *uniform crack location curves*. We observe that a beam without a crack yields a wave fractal dimension of 1.1205, and wave fractal dimension above this nominal value indicates presence of a crack in the beam. Unfortunately, this method can not provide a concrete answer about the severity and location of the crack. However, this method can be used to indicate a combination of size and location of crack or a region of the beam where crack may be present.

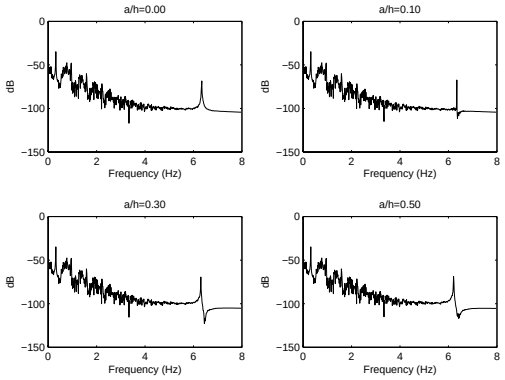

Fig. 11. Power spectrum of beam tip time response for a crack located at $L_1 = 0.2L$

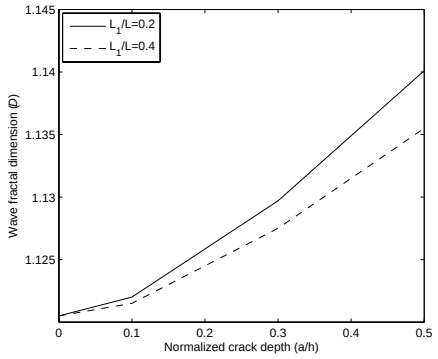

Fig. 12. Wave fractal dimension versus normalized crack depth–uniform crack location curves for $L_1 = 0.2L$ and $L_1 = 0.4L$

Next, to predict the severity and approximate location of the crack on the beam surface, we record the time series data of the beam response along its span for chaotic forcing input. Using the FFT, the time series data is converted to frequency domain. The resulting power spectrum plot is analyzed to identify a suitable window for computing the wave fractal dimension. Throughout this analysis, the frequency window used for computing the wave fractal dimension

is kept fixed for all crack depths considered. Figure 13(a) plots wave fractal dimension against normalized beam length for cracks of various severity located at $L_1 = 0.2L$. These *uniform crack depth curves* yield the same wave fractal dimension till the crack location and their slopes change abruptly at the location of crack. In fact, past the crack location, the uniform crack depth curves exhibits a larger slope for a larger crack depth. Figure 13(b) shows similar behavior for crack location, $L_1 = 0.4L$. The abrupt split in uniform crack depth curves at crack location and their increasing slope with increasing crack depth can be used to establish both the severity and location of crack.

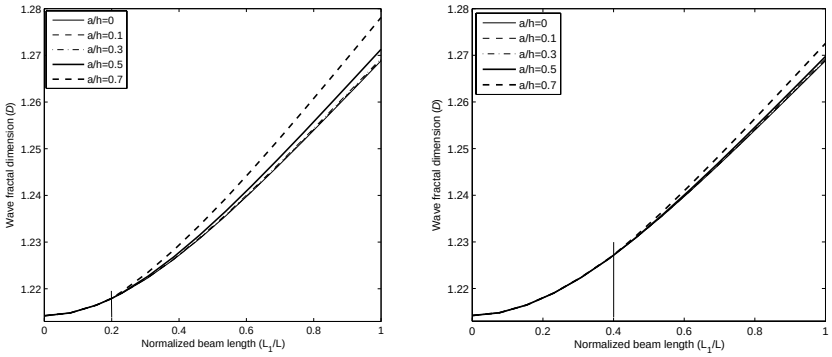

(a) (b)

Fig. 13. Wave fractal dimension versus normalized beam length–uniform crack depth curves for (a) $L_1 = 0.2L$ and (b) $L_1 = 0.4L$

7 Experimental Verification

A schematic of the experimental setup used is given in Figure 14. An aluminum base holds the shaker (Brüel & Kjær Type 4810). To produce a base excitation, a test specimen is clamped on shaker. An accelerometer (Omega ACC 103) is mounted at the tip of the specimen using mounting bee wax. Our software environment consists of Matlab, Simulink, and Real Time Workshop in which the Chen's chaotic oscillator is propagated to obtain the time series corresponding to the y_1 signals of (1). Next, an analog output block in the Simulink program outputs the y_1 signal to a digital to analog converter of Quanser's Q4 data acquisition and control board which in turn is fed to a 12 volt amplifier (Kenwood KAC-8202) to drive the shaker. The accelerometer output is processed by an amplifier (Omega ACC PSI) and interfaced to an analog to digital converter of the Q4 board for feedback to the Simulink program. Properties of the specimen used in our experiments are same as in Section 6. To emulate a fine hair crack, we used a 0.1 mm saw to introduce cracks of several different desired depths. As noted in [3], sawed and cracked beams yield different natural frequencies wherein the frequency difference is dependent on the width of the cut.

Thus, it follows that the frequency characteristics of sawed and cracked beams may differ significantly for larger crack width and render the natural frequency based crack detection methods ineffective. The results of this effort are not significantly affected since, instead of relying on changes in natural frequency, our crack detection approach relies on measuring and comparing wave fractal dimension of chaotically excited vibration response. For specimen of different crack depth, all located at $L_1 = 0.2L = 100$ mm from fixed end, the accelerometer measurement is recorded and used to produce the output response time series, which is used to perform our analysis. A total of six specimens were prepared with crack depth varying from 0% to 50% of the thickness. In all the specimen, saw crack was introduced on the top surface to match with the simulation condition.

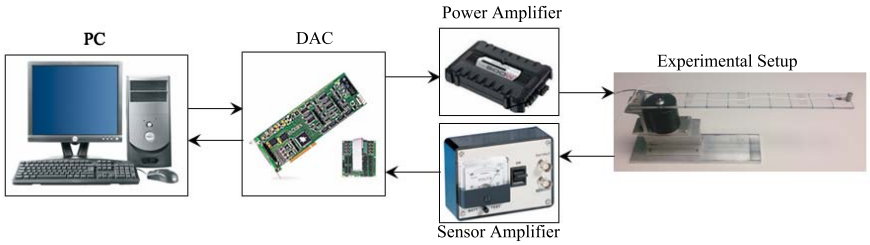

Fig. 14. Experimental setup

The time series data obtained from the accelerometer suffered from general sensor errors (dc offset and ramp bias), causing the raw time series data to be unusable for further analysis. We used the Wavelet transformation toolbox [9] of MATLAB to filter the raw time series data and remove the errors. This filtering technique uses a moving average of the waveform to shift its mean to 0 [6]. Using this technique with Chen's input to the beam structure with various crack depth, we obtain Figure 15 that shows the corrected time series. Next, we use the time series data of Figure 15 to compute the wave fractal dimension and plot the result against the crack depth. Following the trends observed in our numerical study, in Figure 16(a), wave fractal dimension versus crack depth plot shows an increasing trend.

Finally, we perform FFT on the time series data of Figure 15 to obtain the power spectrum plots (see [6]) for various crack depths. Next, we compute the wave fractal dimension of the frequency domain data using a window from 0 to 20 Hz. Figure 16(b) shows that the wave fractal dimension of frequency domain data exhibits an increasing trend against increasing crack depth, matching the trend observed in our numerical study. Although the plots obtained from the experimental data are not as smooth as the ones resulting from numerical simulation, this may be the result of inaccuracies resulting from sample preparation or a variety of experimental errors [6].

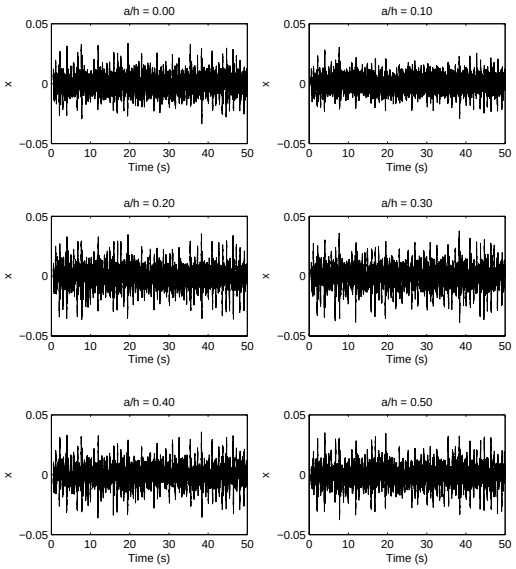

Fig. 15. Filtered time series for different crack depths with Chen's input

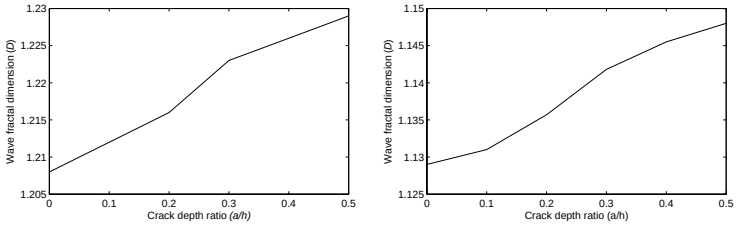

(a) (b)

Fig. 16. Wave fractal dimension for different crack depths at $L_1 = 0.2L$ from (a) time series and (b) frequency domain data

8 Conclusion

In this paper, to detect and characterize a crack in a beam, we considered a SDOF and a FE model of the beam excited by a chaotic force input. We showed that for the SDOF model, crack severity can be easily and consistently predicted by using wave fractal dimension of power spectrum of time series data. Moreover, for the FE model, we showed that wave fractal dimension exhibits a trend that can be used to predict crack location and crack depth. Finally, the simulation results were validated experimentally.

Acknowledgments

This work is supported in part by the National Science Foundation under an RET Site grant 0807286, a GK-12 Fellows grant 0741714, and the NY Space Grant Consortium under grant 48240-7887.

References

1.N. Bouraou and L. Gelman. Theoretical bases of free oscillation method for acoustical non-destructive testing. *Proceedings of Noise Conference, The Pennsylvania State University*, 519–524, 1997.

2.Y. Bamnios, E. Douka, and A. Trochidis. Crack identification in beam structures using mechanical impedance. *Journal of Sound and Vibration*, 256(2):287–297, 2002.

3.P. Cawley and R. Ray. A comparision of natural frequency changes produced by cracks and slots. *Transactions of the ASME*, 110:366–370, 1998.

4.S. Chinchalkar. Determination of crack location in beams using natural frequencies. *Journal of Sound and Vibration*, vol. 247(3), pp. 417–429. 2001.

5.C. H. Duane and L. L. Bruce. Mastering Matlab 7. Upper Saddle River, New Jersey, 2005. Prentice Hall.

6.C. Dubey. Damage Detection in Beam Structures using Chaotic Excitation. Master's Thesis at Polytechnic Institute of NYU, New York, 2010.

7.L. J. Hadjileontiadis, E. Douka, and A. Trochidis. Fractal dimension analysis for crack identification in beam structures. *Mechanical Systems and Signal processing*, vol. 19, pp. 659–674. 2005.

8.L. J. Hadjileontiadis and E. Douka. Crack detection in plates using fractal dimension. *Engineering Structures*, vol. 29, pp. 1612–1625. 2007.

9.A. Jensen and la. CH. Anders. Ripples in Mathematics: The Discrete Wavelet Transform. New York, 2001. Cambridge University Press.

10.J. F. James. A Student's Guide to Fourier Transforms: With Applications in Physics and Engineering. New York, NY, 2003. Springer Verlag.

11.J. T. Kim and N. Stubbs. Crack detection in beam type structures using frequency data. *Journal of Sound and Vibration*, vol. 259(1), pp. 145–160. 2003.

12.M. J. Katz. Fractals and the analysis of waveforms. *Computers in Biology and Medicine*, vol. 18(3), pp. 145–156. 1998.

13.J. Lee. Identification of multiple cracks in a beam using natural frequencies. *Journal of Sound and Vibration*, vol. 320, pp. 482–490. 2009.

14.S. Moaveni. Finite Element Analysis Theory and Application with ANSYS. Upper Saddle River, NJ, 2007. Prentice Hall.

15.J. M. Nichols, S. T. Trickey, and Virgin. Structural health monitoring through chaotic interrogation. *Meccanica*, 38:239–250, 2003.

16.S. Orhan. Analysis of free and forced vibration of a cracked cantilever beam. *NDT&E International*, 40:443–450, 2007.

17.D. P. Patil and S. K. Maiti. Experimental verification of a method of detection of multiple cracks in beams based on frequency measurements. *Journal of Sound and Vibration*, vol. 281, pp. 439–451. 2005.

18.J. Ryue and P. R. White. The detection of crack in beams using chaotic excitations. *Journal of Sound and Vibration*, 307:627–638, 2007.

19.P. F. Rizos, N. Aspragathos, and A. D. Dimarogonas. Identification of crack location and magnitude in a cantilever beam from the vibration modes. *Journal of Sound and Vibration*, 138(3):381–388, 1990.

20.J. C. Sprott. Chaos and Time-Series Analysis. New York, NY, 2003. Oxford University Press.

21.M. Taghi, B. Vakil, M. Peimani, M. H. Sadeghi, and M. M. Ettefagh. Crack detection in beam like structures using genetic algorithms. *Applied Soft Computing*, 8:1150–1160, 2008.

22.I. Trendafilova and E. Manoach. Vibration-based damage detection in plates by using time series analysis. *Mechanical Systems and Signal processing*, 22:1092–1106, 2008.

23.E. Viola, L. Federici, and L. Nobile. Detection of crack using cracked beam element method for structural analysis. *Theoretical and Applied Fracture Mechanics*, vol. 36, pp. 23–35. 2001.